Journal of Agricultural Machinery

Homepage: https://jame.um.ac.ir

Research Article
Vol. 15, No. 3, 2025, p. 275-289

Investigating the Potential of the Innovative YOLOv8s Model for Detecting Bloomed Damask Roses in Open Fields

F. Fatehi [1], **H. Bagherpour** [1*], **J. Amiri Parian** [1]

1- Department of Biosystems Engineering, Faculty of Agriculture, Bu-Ali Sina University, Hamedan, Iran
(*- Corresponding Author Email: h.bagherpour@basu.ac.ir)

Received: 14 May 2024 Revised: 25 July 2024 Accepted: 27 July 2024 Available Online: 31 May 2025	**How to cite this article:** Fatehi, F., Bagherpour, H., & Amiri Parian, J. (2025). Investigating the Potential of the Innovative YOLOv8s Model for Detecting Bloomed Damask Roses in Open Fields. *Journal of Agricultural Machinery, 15*(3), 275-289. https://doi.org/10.22067/jam.2024.88066.1249

Abstract

Manually picking the flowers of the Damask rose is significantly challenging due to the numerous thorns on its stems. Consequently, the accurate detection of bloomed Damask roses in open fields is crucial for designing a robot capable of automating the harvesting process. Considering the high speed and precise capabilities of deep convolutional neural networks (DCNN), the objective of this study is to investigate the effectiveness of the optimized YOLOv8s model in detecting bloomed Damask roses. To assess the impact of the YOLO model size on network performance, the precision and detection speed of other YOLO network versions, including v5s and v6s, were also examined. Images of Damask roses were taken under two lighting conditions: normal light conditions (from civil twilight to sunrise) and intense light conditions (from sunrise to 10 AM). The outcomes demonstrated that YOLOv8s exhibited the highest performance, with a mean average precision (mAP50) of 98% and a detection speed of 243.9 fps. This outperformed the mAP50 and detection speed of YOLOv5s and YOLOv6s networks by margins of 0.3%, 6.1%, 169.3 fps and 198.6 fps, respectively. Experimental results show that YOLOv8s performs better on images taken in normal lighting than on those taken in intense lighting. A decline of 5.2% in mAP50 and 2.4% in detection speed signifies the adverse influence of intense ambient light on the model's effectiveness. This research indicates that the real-time detector YOLOv8s provides a feasible solution for the identification of Damask rose and provides guidance for the detection of other similar plants.

Keywords: Ambient light, Deep learning, Object detection, Rose flower, YOLO

Introduction

Damask rose (*Rosa damascena* mill.) is a precious species of rose and has been extensively used in various cosmetic, health, and pharmaceutical industries. Bulgaria, Turkey, India, and Iran are ranked first through fourth in the cultivation area dedicated to this crop. Furthermore, Bulgaria, Turkey, and Iran hold this plant's top three positions in oil and essential oil production. (Ucar, Kazaz, Eraslan, & Baydar, 2017; Yousefi & Jaimand, 2018).

Harvesting Damask rose is the most labor-intensive aspect of this flower's production. This is due to the rapid emergence of rose blooms, which occur only once a year for a short period of 15 to 20 days. These plants produce numerous bloomed and fully-opened flowers each day, necessitating harvesting from 4:00 AM to 7:00 AM to obtain the highest-quality Damask rose oil in quantity and quality. Most Damask rose buds fully bloom early in the morning and should be harvested on the same day, as withered flowers

https://doi.org/10.22067/jam.2024.88066.1249

that had fully bloomed the previous day are not harvested (Rusanov, Kovacheva, Rusanova, & Atanassov, 2011). In addition to the requirement to harvest fully-bloomed flowers in a narrow window, the harvesting of this crop is inherently difficult and has not yet been fully mastered technologically, so manual harvesting remains the traditional approach. While harvesting the buds, workers may sustain injuries from the thorns on the stems. As such, it is imperative to provide adequate training for these workers. The challenges related to labor, along with the costs and time required for worker training, significantly contribute to the total expense of harvesting this crop (Manikanta, Rao, & Venkatesh, 2017). Consequently, the real-time identification of bloomed Damask rose in open fields is crucial for developing a machine or robot capable of autonomously harvesting Damask roses. One approach to achieving high efficiency in this field involves the utilization of machine vision techniques.

In recent years, convolutional neural networks (CNN) have emerged as novel machine learning methods garnering substantial attention from researchers for flower classification and qualitative evaluations. (Guru, Kumar, & Manjunath, 2011; Wang, Underwood, & Walsh, 2018; Sun, Wang, Liu, & Liu, 2021; Zhang, Su, & Wen, 2021; Bataduwaarachchi *et al.*, 2023). CNN model was designed to detect apple blossoms, which was able to identify apple tree blossoms with an accuracy of over 79%. This model, without the need for retraining, could identify apple, peach, and pear blossoms on the trees with an accuracy of over 67%, 86%, and 94%, respectively (Dias, Tabb, & Medeiros, 2018). Wu, Lv, Jiang, and Song (2020) developed a channel pruning-based YOLOv4 that facilitates the acquisition of apple blossom thinning robots. This model can identify apple blossoms with a mean average precision (mAP) of 97.31% and a detection speed of 72.33 fps, which compared to the base model YOLOv4, reduces the mAP, detection speed, and size by 0.24%, 39.47%, and 231.51 MB, respectively. By pruning low-load weights of model in apple blossom detection using the channel pruning method, they achieved a lighter model. Wang *et al.* (2022) used the developed YOLOv4, called YOLO-PEFL, to estimate the performance of pear orchards through detecting and counting flowers. ShuffleNetv2, embedded by the SENet (Squeeze-and-Excitation Networks) module replacing the original backbone network of the YOLOv4 model, formed the backbone of the YOLO-PEFL model. The empirical findings indicated that the mean accuracy of the YOLO-PEFL framework was 96.71%, the framework's dimensions were decreased by approximately 80%, and the mean recognition velocity was 0.027 s. In comparison to the YOLOv4 framework and the YOLOv4-tiny framework, the YOLO-PEFL framework exhibited superior performance in framework dimensions, recognition precision, and recognition speed, thereby effectively decreasing framework deployment expenditure and enhancing framework effectiveness. YOLO network training using drone-captured images was employed to create a map depicting pumpkin flower distribution in the field. In this research, the mAP50 was 91% (Mithra & Nagamalleswari, 2023). To aid the marketing of roses, Anjani, Pratiwi, and Nurhuda (2021) developed a Convolutional Neural Network (CNN) model capable of categorizing the variety of roses without manual categorization. In this study, the accuracy achieved on the evaluation dataset was 96.33%. Shinoda *et al.* (2023) recognized that strategic planning for cut flower production is pivotal, as demand varies throughout the year. Nevertheless, manual enumeration of all rose blossoms in the greenhouse is time-intensive and arduous. They used YOLOv5 to identify small rose blossoms from various angles during camera motion, diminishing detection inaccuracies and attaining an F1 score of 0.950.

By reviewing the research literature, it has become apparent that there is a gap in the existing literature regarding a thorough examination of the precise and real-time identification of bloomed Damask rose flowers in agricultural fields for the purpose of automating the harvesting process. As a result, the present study aims to address this deficiency by leveraging the potential of deep learning models, specifically focusing on the compact YOLO models, known for their adeptness in accurately and swiftly identifying various types of flowers. In this investigation, upon completion of training the models and fine-tuning their weights, the performance of each individual model was assessed using a collection of images captured during harvest time. To carefully examine the effect of ambient lighting on the detection proficiency of the chosen model, the model underwent training and evaluation using images captured under two distinct lighting conditions: normal light and intense light.

Materials and Methods

Data collection and preparation

In order to extract the optimal essence from high-quality Damask rose petals, it is imperative to harvest these blooms during the early hours of the morning (Kumar, Sharma, Sood, Agnihotri, & Singh, 2013; Thakur, Sharma, & Kumar, 2019). To train models, two distinct sets of videos were acquired from Damascus rose fields situated in the village of Sarab, Dehgolan, Kurdistan Province, Iran. These videos were obtained using a Samsung Galaxy Note 9 smartphone camera during May–June 2022. The first collection of videos, which were labeled "Normal Light Condition," was obtained in the morning from twilight until sunrise. Conversely, the second set, labeled "Intense Light Condition," was acquired from sunrise to 10 AM to assess the impact of intense illumination on the efficacy of the chosen model trained using the aforementioned images (Fig. 1).

In the study conducted by Sharma and Kumar (2018), the six distinct flowering stages of Damask rose were explored. These stages that affect the yield and quality of the essence are: 1) Sepals intact with dark immature petals, 2) Sepals separated from petals, petals whorl closed, 3) Petals whorl loosened, 4) Petal whorl opened, 5) Fully opened flower, and 6) Flower opened the previous day. The outcomes of their study indicated that the early harvest stages of flowers (1, 2, and 3) exhibited variations in scent characteristics when compared to fully bloomed flowers. Moreover, the maximum essential oil content exhibited notable differences across various harvest stages and the duration of hydrodistillation. Notably, at the fourth stage of flowering (fully open petal whorl), along with a hydrodistillation duration of 5 hours, yielded the highest quality of essential oil. Additionally, immature or overly mature flowers not only diminish essential oil yield but also compromise oil quality. Consequently, stages 4 and 5 were identified as the target harvesting stages for rose flowers, classified as bloomed flowers in this study. Fig. 2 depicts different flower opening stages from 1 to 6, as described earlier.

Labeling

The LabelImg v1.8.0 software was utilized for the purpose of annotating images of damask roses. Utilizing this software resulted in the generation of output files saved in the TXT format specifically tailored for YOLO networks. As depicted in Fig. 3, a visual representation is provided, illustrating the contents of the output file pertaining to two individual flowers. Within this illustration, various symbols such as NO, Nc, Xc, Yc, W, and H are utilized to represent specific parameters including the number of objects in the image, the object class, longitudinal and transverse coordinates of the frame's center, width, and height of bounding boxes, respectively. All these values are normalized within a range of zero to one. Given that the main focus of the present study was the identification of bloomed Damask roses, a single class was considered, denoted as "Ripe=0".

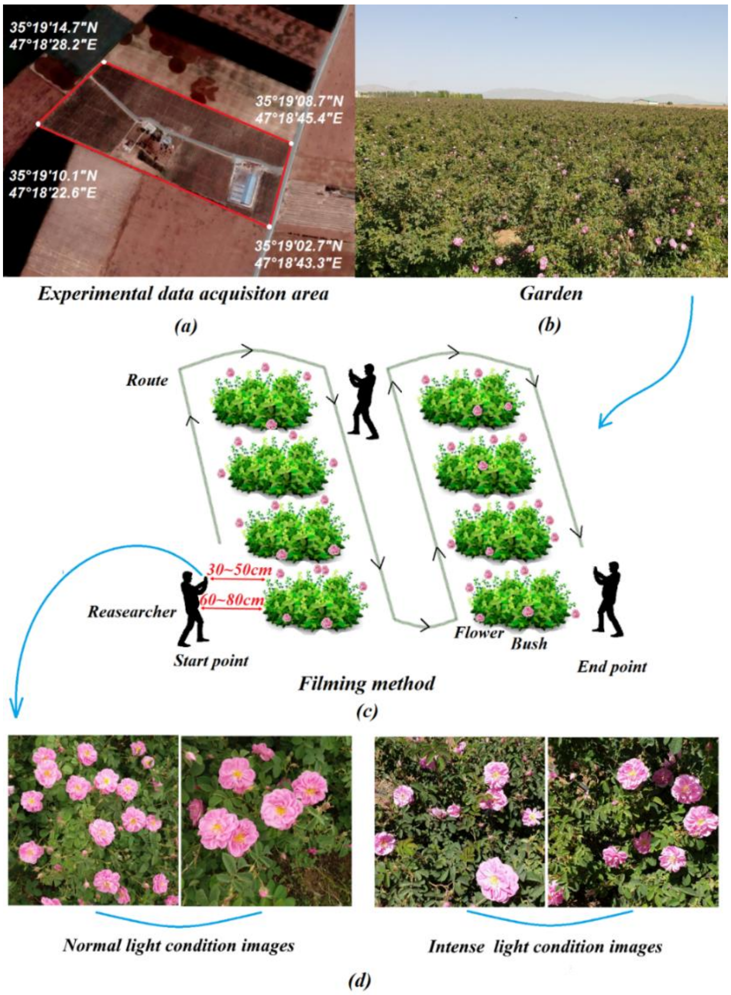

Fig.1. Schematic diagram of the image acquisition process: (a) Geographical coordinates of the garden, (b) The garden, (c) Video capture method, and (d) Example images

Fig.2. Different stages of development of damask rose: (1) sepals intact with dark immature petals, (2) sepals separated from petals, petals whorl closed, (3) petals whorl loosened, (4) petal whorl opened, (5) fully opened flower, and (6) flower opened the day before

In this study, five hundred images were extracted from collected videos. Extracting consecutive frames from the video is essential for the stability of YOLO detection (Tung *et al.*, 2019). To reduce the computational cost and increase the image processing speed and speed up the model training, all images were 512 x 512 pixels. To check the robustness of the model and issues like overfitting and underfitting, a technique called K-fold cross validation was used. We created 10 folds of the dataset, and each fold was executed 5 times. In this study, 10% of images were allocated for testing purposes.

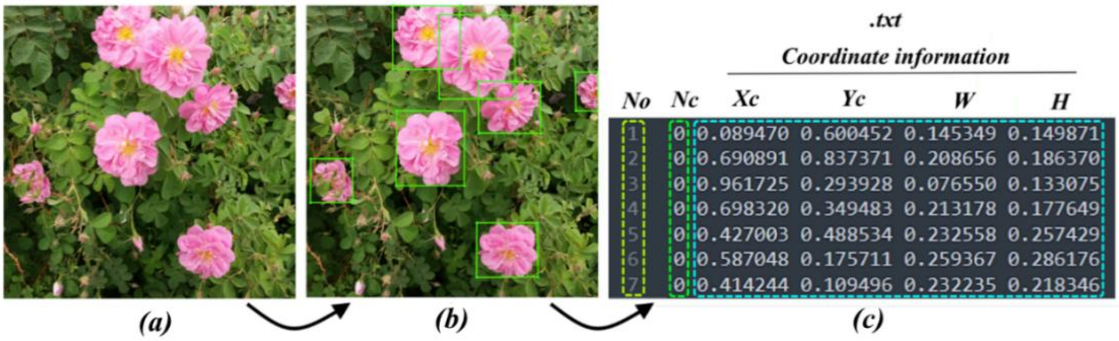

Fig.3. The process of creating the annotation: (a) original Damask rose, (b) labeled desired flowers, and (c) annotation results in .txt format

YOLO Model

The YOLO model has had a notable development in the field of real-time object detection. By employing a convolutional network that evaluates images in a single step, YOLO can detect objects directly and calculate the precise object coordinates. The utilization of this methodological approach has resulted in a substantial enhancement in detection speed (Redmon, Divvala, Girshick, & Farhadi, 2016; Silva, Monteiro, Ferreira, Carvalho, & Corte-Real, 2019).

In January 2023, Ultralytics unveiled the YOLOv8 model, building upon their prior launch of the YOLOv5 model. This latest version represents the pinnacle of advancements in comparison to its predecessors. The YOLOv8 model, which underwent training on ImageNet, demonstrated heightened accuracy and speed of detection in contrast to the YOLOv5 and YOLOv6 models that had undergone similar training (Jocher, Chaurasia, & Qiu, 2023). A comprehensive schematic depiction of the YOLOv8 model can be observed in Fig. 4. This model retains the primary network of YOLOv5, but features a notable modification in its CSP layer, now referred to as the C2f module. The C2f module improves detection accuracy by combining high-level features with contextual information. YOLOv8 is an anchor-free model that employs a distinct head for the autonomous processing of object detection, classification, and regression tasks. This design facilitates each branch's concentration on its respective task, thus enhancing the overall precision of the model. In the output layer of YOLOv8, the sigmoid function serves as the activation function for abjectness, while the softmax function is employed for class probabilities (Terven & Cordova-Esparza, 2023).

Among the different scales of each architecture in the YOLO family, only those meeting the following criteria were chosen: 1- Having a parameter count below 2 million, and 2- Achieving a detection speed of less than 1.5 ms per image on the COCO dataset using a GPU A100. Ultimately, the scale with the highest mAP50-95 value was selected for each architecture, in the YOLO family, only YOLOv8s, YOLOv6s, and YOLOv5s met these criteria (Ultralytics, n.d.).

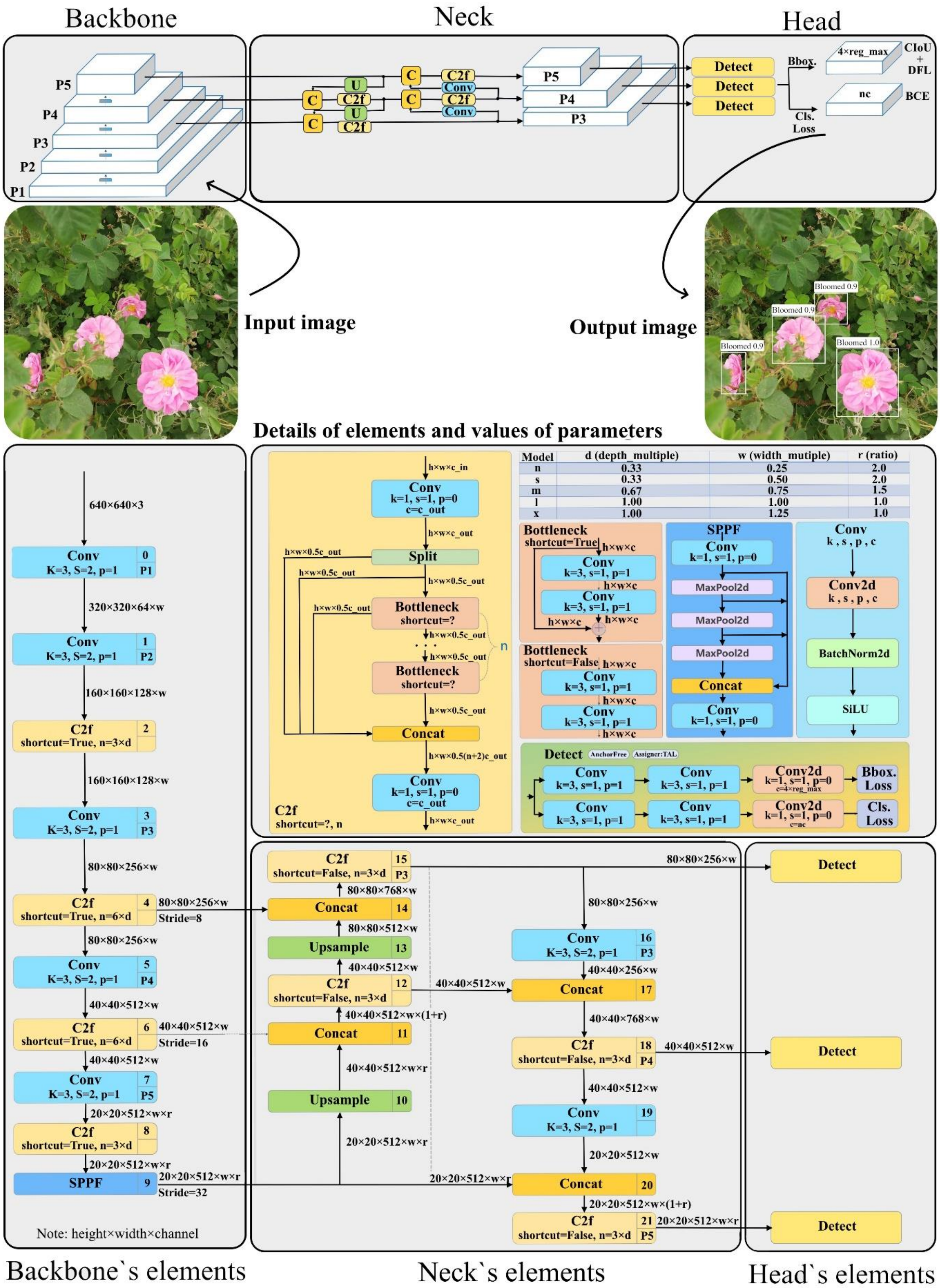

Fig.4. The architecture of YOLOv8 used in the detection of Damask rose

Evaluation Parameters of YOLOv8s

Adjustable parameters of the YOLOv8s model, pre-trained on the COCO val2017 dataset, primarily include changes in input size, batch size, number of classes, learning rate, and number of iterations (Table 1). Additionally, to generalize the model's detection to other farm-like conditions close to the flower harvest timeframe, data augmentation techniques were utilized during training. By adjusting hyperparameters related to these techniques, changes were made in the color values (HSV color space), image brightness, clarity, and images were rotated and flipped in different directions.

Table 1- Parameters of YOLOv8s for *Rosa damascena mill* flower detection

Parameter	Value
Input size	512×512
Learning rate	1×10^{-3}
Batch size	32
Classes	1
Epochs	75

A loss function is a mathematical function that quantifies the difference between predicted and actual values in a machine learning model. According to Equations 1 to 8, the loss function in the training of YOLO models mainly comprised three sections: the bounding box location loss (L_{CIoU}), the confidence loss ($L_{confidence}$), and the class loss (L_{class}) (Wu *et al.*, 2020):

$$Loss = L_{CIoU} + L_{confidence} + L_{class} \quad (1)$$

$$Loss_{CIoU} = 1 - IoU + \frac{d^2}{c^2} + \alpha\nu \quad (2)$$

$$L_{confidence} = \sum_{i=0}^{S^2}\sum_{j=0}^{B} K[-\log(p) + BCE(\hat{n}, n)] \quad (3)$$

$$L_{class} = \sum_{i=0}^{S^2}\sum_{j=0}^{B} 1_{i,j}^{noobi}[-\log(1-p_C)] \quad (4)$$

$$BCE(\hat{n}, n) = -\hat{n}\log(n)-(1-\hat{n})\log(1-n) \quad (5)$$

$$\alpha = \frac{\nu}{(1-IoU)+\nu} \quad (6)$$

$$\nu = \frac{4}{\pi^2}(\tan^{-1}\frac{w^{gt}}{h^{gt}} - \tan^{-1}\frac{w}{h})^2 \quad (7)$$

$$K=1_{i,j}^{obj} \quad (8)$$

IoU is defined as the ratio of the intersection and union of the predicted bounding box and the ground truth bounding box, with *c* and *d* denoting the distances between the centers of the two bounding boxes and the diagonal distance of their union, respectively. The parameters w^{gt} and h^{gt} represent the width and height of the ground truth bounding box, while w and h correspond to the width and height of the predicted bounding box. The variable *S* stands for the number of grids, while *B* signifies the anchor number associated with each grid. *K* is a symbol for weight, taking the value of 1 in case there is an object in the j-th anchor of the i-th grid; otherwise, it is 0. Moreover, $\hat{n}$ and *n* indicate the actual and predicted classes of the j-th anchor in the i-th grid, and *p* represents the probability of the object being a Damask rose flower. The mean average precision (mAP), precision, recall, F1 score, F2 score, and detection speed were employed to assess the efficacy of the models:

$$mAP = \frac{\sum_{c=1}^{C} AP(C)}{C} \quad (9)$$

$$Precision = \frac{TP}{TP+FP} \times 100\% \quad (10)$$

$$Recall = \frac{TP}{TP+FN} \times 100\% \quad (11)$$

$$F1 = 2 \times \frac{Precision \times Recall}{Precision + Recall} \times 100\% \quad (12)$$

$$F2 = 5 \times \frac{Precision \times Recall}{4 \times Precision + Recall} \times 100\% \quad (13)$$

where *c* refers to the number of classes (here, *c* = 1), and TP, FP, FN, and TN are true positive (the bloomed flowers that are correctly classified as bloomed flower), false positive (a region of background that is classified as a bloomed flower), false negative (the bloomed flowers that are considered as background), and true negative (defined as all background areas in the image except for regions where bloomed flowers are present), respectively.

Results and Discussion

Comparison of different detection algorithms

Fig. 5 depicts the training mAP50 of four models on images captured under normal light conditions. The training curve for the four models indicated that the YOLOv8s model reached saturation faster than the other models, exhibited lower fluctuations, and maintained a more uniform curve. Table 2 presents the performance results of the YOLOv8s model compared with the YOLOv5s and YOLOv6s models regarding detecting bloomed Damask roses. Based on the results, the mAP50 scores for the three object detection models were as follows: 0.98%, 93.9%, and 97.7%, respectively. According to these results, YOLOv8s demonstrated the highest mAP50 among the three models. A preliminary analysis suggested that the CSPDarknet53 feature extractor, as a backbone of the YOLOv8-Seg model, which is followed by a novel C2f module instead of the traditional YOLO neck architecture, is more competent in extracting diverse and complex features of targets, playing a fundamental role in the detection accuracy improvement of YOLOv8.

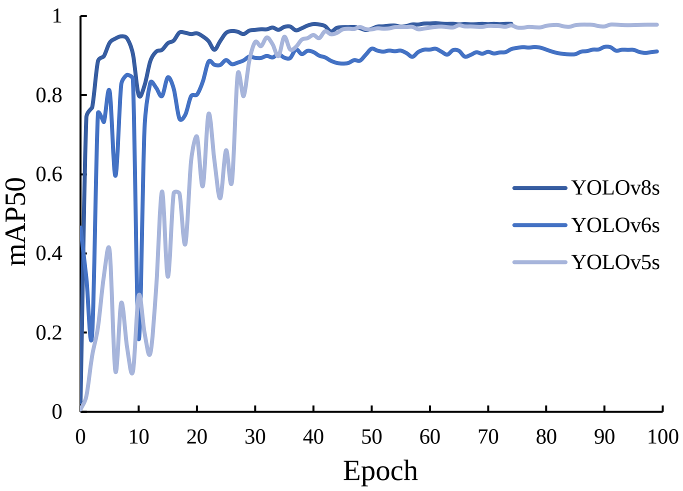

Fig.5. Comparing mAP50 of different YOLO models obtained from the training dataset

Table 2- Performance results of various models in the detection of Damask roses

Algorithm	Recall (%)	Precision (%)	mAP50 (%)	Detection speed (fps)	F1 (%)	F2 (%)	Model size (MB)
YOLOv8s	93.7	97.3	98.0	243.9	95.5	94.4	21.5
YOLOv6s	84.7	88.2	93.9	45.3	86.4	85.4	41.3
YOLOv5s	94.1	95.1	97.7	74.6	94.6	94.3	14.1

The analysis of the results indicates that all models demonstrated high precision in detecting the bloomed Damask roses. Notably, the YOLOv8s model exhibited superior precision at 98% and a remarkable detection speed of 243.9 fps, outperforming the other models. In contrast, the YOLOv5s model, while achieving a close precision rate of 97.7% compared to the YOLOv8s model and having a smaller size of 14.1 MB, exhibited a significantly lower detection speed, being 3.27 times slower. This underscores the YOLOv8s model's exceptional suitability for real-time detection tasks. Worth noting is that the YOLOv6s model achieved a detection precision of 88.2%. Nevertheless, its applicability for real-time and robotic tasks was limited due to its low detection speed of 45.3 fps and a substantial size of 41.3 MB (Wu *et al.,* 2020). This limitation is especially significant considering that the frame rate of most videos is 30 fps, and economic robot controllers typically possess limited memory capacity. The YOLOv5s model was explicitly designed for real-time detection tasks like apple thinning and crop yield estimation before thinning. Its parameters and size were optimized through channel pruning and weight adjustments. Consequently, boasting a size of 1.4 MB and a detection speed of 125 fps, this model performed well (Wang & He, 2021).

Furthermore, the YOLOv8s model, with its enhanced attributes of precision, speed (198.6 fps), and smaller size (19.8 MB), surpassed the YOLOv6s model in all aspects. This positions the proposed model as an ideal choice for real-time detection of bloomed Damask rose, effectively addressing the challenges associated with precision, size, and speed. Consequently, it can be seamlessly integrated into mobile phone applications or employed in Damask rose harvesting robots.

The efficacy of various versions of the YOLO model is impacted by their scale (quantified by the number of parameters), as well as the dataset employed for both training and evaluation. Hence, it is essential to assess the performance of the intended models. Apeinans *et al.* (2024) created a cherry dataset (CherryBBCH81) for training neural networks. They aimed to find the best YOLO model for fruit detection. YOLOv5m performed better with the CherryBBCH81, achieving a mAP50 of 0.886, compared to YOLOv8m with 0.870. However, YOLOv8m showed better results with the Pear640 dataset, reaching 0.951 compared to 0.943 for YOLOv5m. Estrada, Vasconez, Fu, and Cheein (2024) tested YOLO models 5, 7, and 8 of various sizes (n, s, m, l, and x) for peach fruit detection. The findings indicated that YOLO version 7 X model exhibited the highest performance.

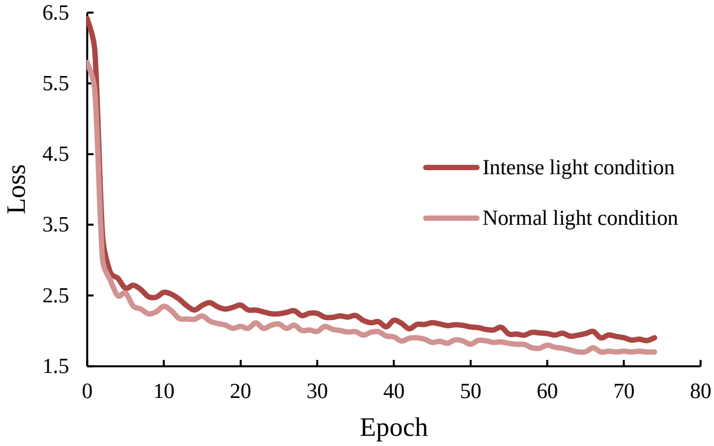

Fig.6. Loss of training YOLOv8s

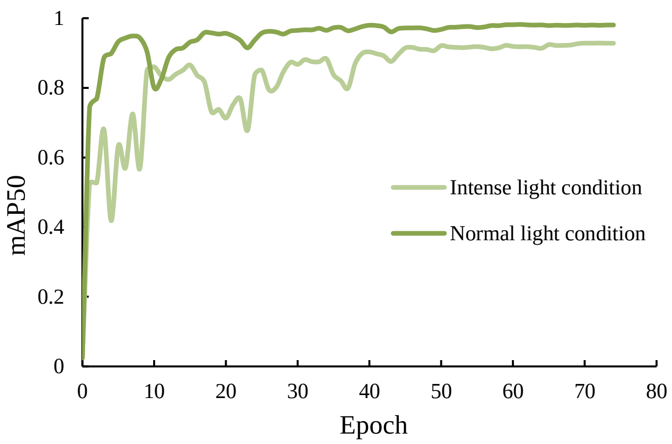

Fig.7. mAP50 of training YOLOv8s

Ambient light effect on YOLOv8s performance

Figs. 6 and 7 display the model's loss

curves and mAP50 during training, based on two images taken under normal and intense light conditions. The visual data from these figures reveals that when Damask rose bushes were blooming, the model showed increased learning efficiency and faster convergence in the early stages of object detection training. However, as time passed, the learning curve gradually flattened, indicating a slower rate of improvement until the model's learning efficiency reached a saturation point through deep learning processes. It is also important to note that the loss function stabilized at a constant value after the 64th epoch for normal light and the 71st training epoch for intense light. This indicates that the training process has been completed, resulting in a stable and well-optimized detection model.

The Fig. 8 illustrates the confusion matrix obtained from the YOLOv8s results related to the data of normal and intense light conditions. The confusion matrix of this model highlights the potential of this method in the detection of bloomed flowers under normal light conditions. As this confusion matrix shows, just fifteen flowers (6.6%) were classified incorrectly as background, whereas under intense light conditions, 31 (13%) samples were incorrectly classified as background. The results of these matrices indicated the negative impact of intense lighting conditions on model performance.

To analyze and compare the performance of DCNN models, four important metrics, such as precision, recall, F1, and F2, were extracted from these figures based on equations 10 to 13, respectively.

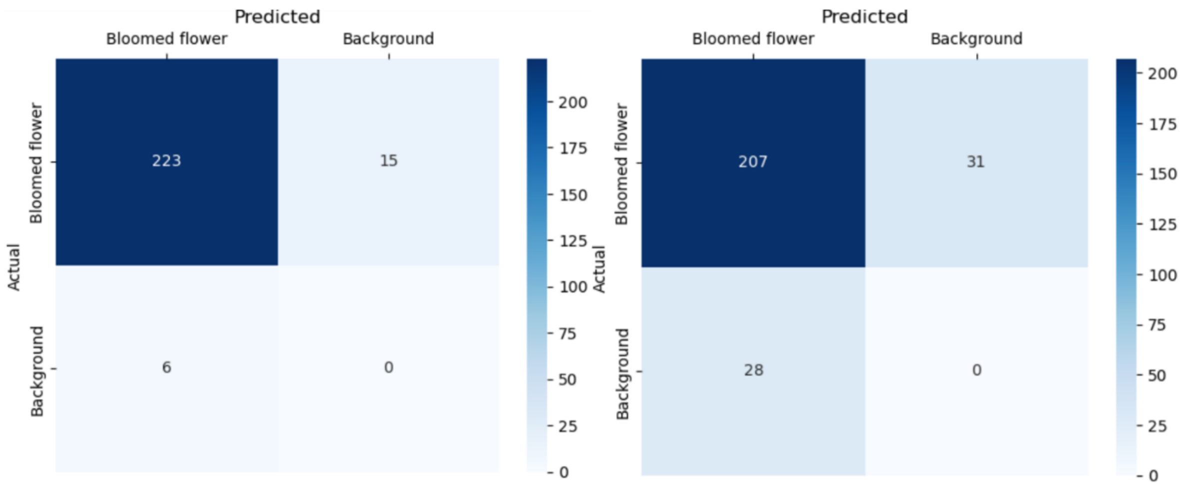

a b

Fig.8. Confusion matrix of YOLOv8s for: (a) normal, and (b) intense light conditions

Table 3 presents the YOLOv8s model training results on two images on normal and intense light conditions. In this table, the performance metrics for images captured under normal light conditions were as follows: mAP50 at 98%, precision at 97.3%, recall at 93.7%, F1 at 95.5%, and F2 at 94.4%. For images taken under intense light conditions, the corresponding metrics were mAP50 at 92.8%, precision at 88.1%, recall at 86.8%, F1 at 93%, and F2 at 87.1%. Additionally, the detection speed reached 243.9 and 238.1 fps, respectively The data presented in this table suggests that the model performed significantly better under normal lighting conditions, indicating that sunlight adversely impacts its effectiveness. In general, the results of this research can be used in the open field. However, we cannot infer that other object detection tasks will exhibit similar mAP to the present study.

Tung *et al.* (2019) have pinpointed that Ultralytics utilizes images sourced from COCO, ImageNet, and various datasets, with a primary focus on solitary objects positioned at the center of the image, for the purpose of training and assessing YOLO models. These images have been acquired through the utilization of diverse cameras featuring distinct configurations, positioned at varying distances and under different lighting conditions. The findings presented by this company are unable to comprehensively capture the potential influence of environmental variables, such as lighting conditions, on the efficacy of the models. Consequently, they have demonstrated the impact of ambient light on the performance of YOLO models.

Table 3- Detection results of Damask roses by YOLOv8s

Light condition	Evaluation index					
	Recall (%)	**Precision (%)**	**mAP50 (%)**	**Detection speed (fps)**	**F1 (%)**	**F2 (%)**
Normal (twilight to sunrise)	93.7	97.3	98.0	243.9	95.5	94.4
Intense (sunrise to 10 AM)	86.8	88.1	92.8	238.1	93	87.1

Fig.9. (a, b) Original images, and (c, d) the results of YOLOv8s in detecting desired Damask rose flowers

Fig. 9 visually illustrates the output of the YOLOv8s for two input images. In addition to ambient lighting conditions, which can impact the precision and speed of bloomed Damask rose detection, various other factors must also be considered. These factors include the meticulous care of flowers, variations in background, deployment, orientation, flower size, distance from the camera, potential obstructions by factors like foliage and other flowers, and the presence of only a few flowers in specific frames. These complexities can sometimes confuse researchers and experts when labeling the flowers, as depicted in Fig. 10. In this figure, flower number 2 was wrongly detected as fully bloomed, whereas flower number 1 was not identified due to being blocked by leaves.

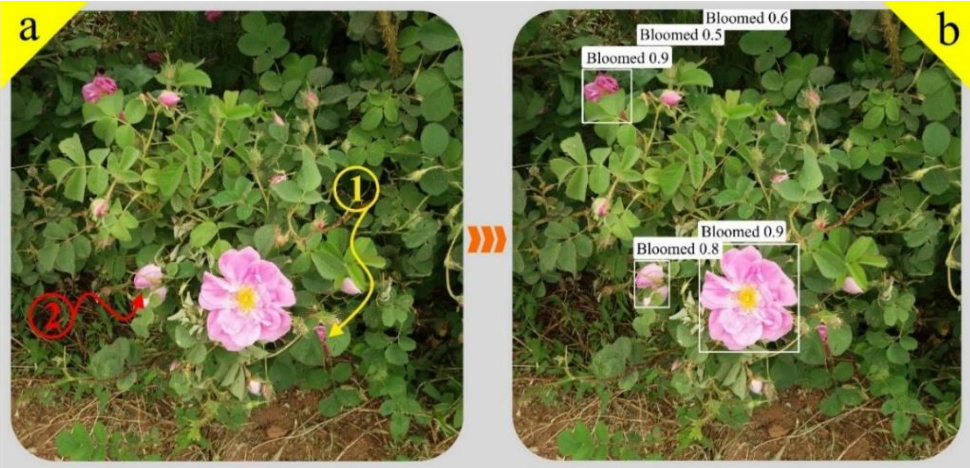

Fig.10. (a) Original image, and (b) result of target detection by YOLOv8s; a flower that (1) could not be detected or (2) was wrongly detected

Conclusion

In this study, the YOLOv8s detection model was introduced for the real-time identification of bloomed Damask rose plants in natural field settings. The principal findings of the investigation were highlighted, revealing the model's remarkable capabilities in achieving high precision and real-time detection of bloomed Damask rose plants. Specifically, when data collected under normal light conditions were applied, an impressive precision rate of 98% was exhibited by the model, underscoring the influence of ambient lighting conditions, which can introduce noise during the detection process. The YOLOv8s model was found to outperform YOLOv5s and YOLOv6s models in terms of both size and detection performance, presenting a more compact footprint while superior detection speed and precision were maintained. Consequently, the YOLOv8s model is well-suited for integration into mobile applications, such as crop yield estimation and the operation of Damask rose harvesting robots, by which it can be utilized. This study highlights the efficacy and practicality of the YOLOv8s detection model for real-time detection tasks in agriculture, particularly for the precise identification of bloomed Damask rose flowers, and it is positioned as a valuable tool for enhancing the efficiency of crop management and automation tasks in Damask rose harvesting.

Conflict of Interest: The authors declare no competing interests.

Authors Contribution

F. Fatehi: Conceptualization, Methodology, Software services, Validation, Data acquisition, Writing original draft preparation.

H. Bagherpour: Supervision, Conceptualization, methodology, Technical advice, Validation, Text mining, Review and editing.

J. Amiri Parian: Review and editing.

References

1. Anjani, I. A., Pratiwi, Y. R., & Nurhuda, S. N. B. (2021, March). Implementation of deep learning using convolutional neural network algorithm for classification rose flower. In *Journal of Physics: Conference Series* (Vol. 1842, No. 1, p. 012002). IOP Publishing. https://doi.org/10.1088/1742-6596/1842/1/012002
2. Apeinans, I., Sondors, M., Litavniece, L., Kodors, S., Zarembo, I., & Feldmane, D. (2024,

June). Cherry Fruitlet Detection using YOLOv5 or YOLOv8? In *ENVIRONMENT. TECHNOLOGIES. RESOURCES. Proceedings of the International Scientific and Practical Conference* (Vol. 2, pp. 29-33). https://doi.org/10.17770/etr2024vol2.8013

3. Bataduwaarachchi, S. D., Sattarzadeh, A. R., Stewart, M., Ashcroft, B., Morrison, A., & North, S. (2023). Towards autonomous cross-pollination: Portable multi-classification system for in situ growth monitoring of tomato flowers. *Smart Agricultural Technology*, *4*, 100205. https://doi.org/10.1016/j.atech.2023.100205
4. Dias, P. A., Tabb, A., & Medeiros, H. (2018). Apple flower detection using deep convolutional networks. *Computers in Industry*, 99, 17-28. https://doi.org/10.1016/j.compind.2018.03.010
5. Estrada, J. S., Vasconez, J. P., Fu, L., & Cheein, F. A. (2024). Deep Learning based flower detection and counting in highly populated images: A peach grove case study. *Journal of Agriculture and Food Research*, *15*, 100930. https://doi.org/10.1016/j.jafr.2023.100930
6. Guru, D. S., Kumar, Y. S., & Manjunath, S. (2011). Textural features in flower classification. *Mathematical and Computer Modelling*, *54*(3-4), 1030-1036. https://doi.org/10.1016/j.mcm.2010.11.032
7. Jocher, G., Chaurasia, A., & Qiu, J. (2023). YOLO by Ultralytics. https://github.com/ultralytics/ultralytics
8. Kumar, R., Sharma, S., Sood, S., Agnihotri, V. K., & Singh, B. (2013). Effect of diurnal variability and storage conditions on essential oil content and quality of damask rose (*Rosa damascena* Mill.) flowers in north western Himalayas. *Scientia Horticulturae*, *154*, 102-108. https://doi.org/10.1016/j.scienta.2013.02.002
9. Manikanta, Y. E. R. R. A. P. O. T. H. U., Rao, S. S., & Venkatesh, R. (2017). The design and simulation of rose harvesting robot. *International Journal of Mechanical and Production Engineering Research and Development*, *9*(1), 191-200.
10. Mithra, S., & Nagamalleswari, T. Y. J. (2023). Cucurbitaceous family flower inferencing using deep transfer learning approaches: CuCuFlower UAV imagery data. *Soft Computing*, *27*(12), 8345-8356. https://doi.org/10.1007/s00500-023-08186-w
11. Redmon, J., Divvala, S., Girshick, R., & Farhadi, A. (2016). You only look once: Unified, real-time object detection. In *Proceedings of the IEEE conference on computer vision and pattern recognition* (pp. 779-788).
12. Rusanov, K., Kovacheva, N., Rusanova, M., & Atanassov, I. (2011). Traditional Rosa damascena flower harvesting practices evaluated through GC/MS metabolite profiling of flower volatiles. *Food Chemistry*, *129*(4), 1851-1859. https://doi.org/10.1016/j.foodchem.2011.05.132
13. Sharma, S., & Kumar, R. (2018). Influence of Harvesting Stage and Distillation Time of Damask Rose (*Rosa damascena* Mill.) Flowers on Essential Oil Content and Composition in the Western Himalayas. *Journal of Essential Oil-Bearing Plants*, *21*(1), 92-102. https://doi.org/10.1080/0972060X.2017.1399089
14. Shinoda, R., Motoki, K., Hara, K., Kataoka, H., Nakano, R., Nakazaki, T., & Noguchi, R. (2023). RoseTracker: a system for automated rose growth monitoring. *Smart Agricultural Technology*, 100271. https://doi.org/10.1016/j.atech.2023.100271
15. Silva, G., Monteiro, R., Ferreira, A., Carvalho, P., & Corte-Real, L. (2019). Face detection in thermal images with YOLOv3. In *Advances in Visual Computing: 14th International Symposium on Visual Computing, ISVC 2019, Lake Tahoe, NV, USA, October 7–9, 2019, Proceedings, Part II 14* (pp. 89-99). Springer International Publishing. https://doi.org/10.1007/978-3-030-33723-0_8
16. Sun, K., Wang, X., Liu, S., & Liu, C. (2021). Apple, peach, and pear flower detection using semantic segmentation network and shape constraint level set. *Computers and Electronics in Agriculture*, *185*, 106150. https://doi.org/10.1016/j.compag.2021.106150

17. Terven, J., & Cordova-Esparza, D. (2023). A comprehensive review of YOLO: From YOLOv1 to YOLOv8 and beyond. *arXiv preprint arXiv:2304.00501*. https://doi.org/10.3390/make5040083
18. Thakur, M., Sharma, S., Sharma, U., & Kumar, R. (2019). Study on effect of pruning time on growth, yield and quality of scented rose (*Rosa damascena* Mill.) varieties under acidic conditions of western Himalayas. *Journal of Applied Research on Medicinal and Aromatic Plants*, *13*, 100202. https://doi.org/10.1016/j.jarmap.2019.100202
19. Tung, C., Kelleher, M. R., Schlueter, R. J., Xu, B., Lu, Y. H., Thiruvathukal, G. K., ... & Lu, Y. (2019, March). Large-scale object detection of images from network cameras in variable ambient lighting conditions. In *2019 IEEE Conference on Multimedia Information Processing and Retrieval (MIPR)* (pp. 393-398). IEEE. https://doi.org/10.1109/MIPR.2019.00080
20. Ucar, Y., Kazaz, S., Eraslan, F., & Baydar, H. (2017). Effects of different irrigation water and nitrogen levels on the water use, rose flower yield and oil yield of *Rosa damascena*. *Agricultural Water Management*, *182*, 94-102. https://doi.org/10.1016/j.agwat.2016.12.004
21. Ultralytics. (n.d.). YOLOv8: Model architecture. Retrieved from https://docs.ultralytics.com/models/yolov8/
22. Wang, C., Wang, Y., Liu, S., Lin, G., He, P., Zhang, Z., & Zhou, Y. (2022). Study on pear flowers detection performance of YOLO-PEFL model trained with synthetic target images. *Frontiers in Plant Science*, *13*. https://doi.org/10.3389/fpls.2022.911473
23. Wang, Z., Underwood, J., & Walsh, K. B. (2018). Machine vision assessment of mango orchard flowering. *Computers and Electronics in Agriculture*, *151*, 501-511. https://doi.org/10.1016/j.compag.2018.06.040
24. Wang, D., & He, D. (2021). Channel pruned YOLO V5s-based deep learning approach for rapid and accurate apple fruitlet detection before fruit thinning. *Biosystems Engineering*, *210*, 271-281. https://doi.org/10.1016/j.biosystemseng.2021.08.015
25. Wu, D., Lv, S., Jiang, M., & Song, H. (2020). Using channel pruning-based YOLO v4 deep learning algorithm for the real-time and accurate detection of apple flowers in natural environments. *Computers and Electronics in Agriculture*, *178*, 105742. https://doi.org/10.1016/j.compag.2020.105742
26. Yousefi, B., & Jaimand, K. (2018). Chemical variation in the essential oil of Iranian *Rosa damascena* landraces under semi-arid and cool conditions. *International Journal of Horticultural Science and Technology*, *5*(1), 81-92. https://doi.org/10.22059/ijhst.2018.256329.234
27. Zhang, M., Su, H., & Wen, J. (2021). Classification of flower image based on attention mechanism and multi-loss attention network. *Computer Communications*, *179*, 307-317. https://doi.org/10.1016/j.comcom.2021.09.001

نشریه ماشین‌های کشاورزی
https://jame.um.ac.ir

مقاله پژوهشی
جلد ۱۵، شماره ۳، پاییز ۱٤۰٤، ص ۲۸۹-۲۷۵

بررسی پتانسیل مدل نوآورانه YOLOv8s در شناسایی گل‌های محمدی شکفته در مزرعه روباز

فرهاد فاتحی [۱]، حسین باقرپور [۱*]، جعفر امیری پریان [۱]

تاریخ دریافت: ۱۴۰۳/۰۲/۲۵
تاریخ پذیرش: ۱۴۰۳/۰۵/۰۶

چکیده

چیدن دستی گل‌های محمدی به دلیل وجود خارهای زیاد روی ساقه‌های آن بسیار دشوار است. بنابراین تشخیص بی‌درنگ گل محمدی شکفته در مزارع روباز برای طراحی یک ربات به‌منظور برداشت خودکار این گل ضروری است. با توجه به سرعت بالا و دقت مناسب شبکه‌های عصبی کانولوشن عمیق (DCNN)، هدف از این مطالعه بررسی پتانسیل مدل بهینه‌شده YOLOv8s در تشخیص گل‌های محمدی شکفته است. به‌منظور ارزیابی اندازه مدل YOLO بر عملکرد مدل، دقت و سرعت تشخیص نسخه‌های دیگر مدل YOLO ازجمله v5s و v6s نیز مورد بررسی قرار گرفت. برای رسیدن به این هدف، تصاویر گل‌های محمدی تحت شرایط نور عادی (از سپیده‌دم تا طلوع آفتاب) و شرایط نور شدید (از طلوع آفتاب تا ۱۰ صبح) تهیه شدند. نتایج ارزیابی نشان داد که مدل YOLOv8s با میانگین متوسط دقت (mAP50) و سرعت شناسایی به‌ترتیب ۹۸٪ و ۲۴۳/۹ فریم در ثانیه (fps) بهترین عملکرد را به نمایش گذاشت و در مقایسه با مدل‌های YOLOv5s و YOLOv6s مقدار mAP50 آن به‌ترتیب ۰/۳ ٪ و ۶/۱ ٪، و مقدار سرعت تشخیص آن به‌ترتیب fps ۱۶۹/۳ و fps ۱۹۸/۶ بیشتر بود. نتایج تجربی نشان می‌دهد که YOLOv8s در تصاویر گرفته‌شده در نور عادی عملکرد بهتری نسبت به تصاویر گرفته‌شده در نور شدید دارد. کاهش ۵/۲ ٪ در مقدار mAP50 و ۲/۴ ٪ در سرعت تشخیص نشان‌دهنده تأثیر منفی نور شدید محیطی بر اثر بخشی مدل است. این تحقیق نشان می‌دهد که مدل YOLOv8s یک راه‌حل قابل‌قبول برای تشخیص بی‌درنگ گل محمدی فراهم می‌کند و راهنمای خوبی برای تشخیص سایر گیاهان مشابه است.

واژه‌های کلیدی: تشخیص اشیا، گل رز، نور محیطی، یادگیری عمیق، YOLO

۱- گروه مهندسی بیوسیستم، دانشکده کشاورزی، دانشگاه بوعلی سینا، همدان، ایران
(*- نویسنده مسئول: Email: h.bagherpour@basu.ac.ir)

https://doi.org/10.22067/jam.2024.88066.1249